Available online at www.sciencedirect.com
SCIENCE DIRECT
Journal of Power Sources 143 (2005) 158–165
JOURNAL OF POWER SOURCES
www.elsevier.com/locate/jpowsour

Radiation heat transfer in SOFC materials and components

David L. Damm, Andrei G. Fedorov*

Woodruff School of Mechanical Engineering, Georgia Institute of Technology, Atlanta, GA 30332-0405, USA

Received 5 November 2004; accepted 27 November 2004
Available online 5 February 2005

Abstract

Radiative transport within the electrode and electrolyte layers, as well as surface-to-surface radiation within the fuel and oxygen flow channels, has the potential to dramatically influence temperature fields and overall operating conditions of solid oxide fuel cells (SOFCs). On a larger scale, radiation from the stack to the environment, including heat losses through insulation, must be accounted for in the plant design, and is of critical importance for effective thermal management of the high temperature stack. In this report, we discuss the current state-of-the-art and the challenges that remain in understanding, predicting, and quantifying the effects of radiation in SOFC materials and systems. These phenomena are of great interest and importance not only from a fundamental perspective but also from a systems design point of view. Last, but not the least in importance, the determination of radiative properties of the materials involved – either through experimental methods or predictive models – must be an ongoing effort as new materials are continuously being developed.

Keywords: Solid oxide fuel cell; Thermal modeling; Radiation heat transfer; High temperature insulation

1. Introduction

Solid oxide fuel cells (SOFCs) operate at temperatures of the order of 600–1000 °C [1]; thus, radiation heat transfer must be given special consideration in thermal modeling efforts, including stack thermal management and materials development. During the last decades, a number of increasingly detailed theoretical and numerical models of the coupled electro-chemical, thermal, and fluid processes in SOFCs have been developed, and multiple papers have been published on the subject. The first modeling efforts were highly simplified and limited to predicting average cell values such as voltage, current density, and temperature in isothermal cells—which sidesteps the issue of thermal radiation altogether. More detailed, non-isothermal numerical models (for example, [2–4]) began to appear in the early 1990s, and building on these pioneering works, Hartvigsen et al. [5] were the first to consider surface-to-surface radiation exchange in thermal models of SOFCs and concluded that it was significant. Since that time, many papers have reported results of numerical calculations, some including the effects of radiation (for example, see references [6–12]), and others not. The methodologies employed vary from highly simplified analysis to much more detailed, computationally expensive methods (often via commercial CFD codes) with sometimes conflicting results and conclusions reported. Our goal here is to attempt to establish a more complete picture of how radiation heat transfer should be treated in different components of SOFCs and review the justifiable simplifying assumptions that ease the computational burden without compromising the validity of the analysis. We begin with the discussion of radiative heat transfer in semi-transparent anode (positive electrode)–electrolyte–(negative electrode) cathode, or simply, PEN structure of the SOFC unit cell, extend the discussion to surface-to-surface radiation exchange in the flow (air and fuel supply) channels, and finally conclude with the analysis of stack level thermal radiation effects including high temperature thermal insulation and overall stack thermal management.

* Corresponding author. Tel.: +1 404 385 1356; fax: +1 404 894 8496.
E-mail address: andrei.fedorov@me.gatech.edu (A.G. Fedorov).

0378-7753/$ – see front matter © 2005 Elsevier B.V. All rights reserved.
doi:10.1016/j.jpowsour.2004.11.063

Nomenclature

dF	differential view factor
$E_{b\lambda}$	blackbody emissive power ($W\,m^{-2}\,\mu m^{-1}$)
H_0	incident radiation ($W\,m^{-2}\,\mu m^{-1}$)
I_λ	spectral intensity of radiation ($W\,m^{-2}\,\mu m^{-1}$)
n	refractive index of medium
q_λ	spectral radiative heat flux ($W\,m^{-2}\,\mu m^{-1}$)
q_r	total radiative heat flux ($W\,m^{-2}$)
Tr	transmittance of medium

Greek letters

β	extinction coefficient (m^{-1})
ε	emissivity of boundary
κ	absorption coefficient (m^{-1})
λ	wavelength (μm)
ρ	reflectivity
σ	Stefan–Boltzmann constant ($J\,K^{-4}\,m^{-2}\,s^{-1}$)
σ_s	scattering coefficient of medium
τ_λ	spectral optical thickness
τ_L	total optical length of a medium
ω	single scattering albedo
Φ	scattering phase function

From a heat transfer perspective, the unit cell operates as a heat exchanger, dissipating heat generated by the irreversible electrochemical conversion of fuel (hydrogen or reformate in the case of SOFC with internal hydrocarbon fuel reformation) to electricity. On the cathode side, oxygen molecules diffuse through the porous electrode and are reduced at the interface of the cathode and electrolyte. These ions travel through the electrolyte and combine with dissociated hydrogen (at the electrolyte–anode interface), which has diffused through the anode from the fuel channel [1] (see Fig. 1). The irreversibilities of electrochemical reactions and the electrical resistance to flow of ions through the electrolyte generate heat, which is carried out of the cell by the flowing gases in the channels. The heat transfer from this region of generation to the ultimate heat sink (ambient) involves radiative transfer in participating media such as electrodes, electrolyte, and participating gases in the channels, as well as surface-to-surface radiation exchange in the channels.

On the other hand, in a stack of many unit cells, it is desirable to maintain uniform temperature profiles and not allow cells near the edges to operate at lower temperatures than cells in the interior of the stack. Thus, management of heat losses from the stack, through the insulation, to the environment, is of critical importance in maintaining the overall efficiency of the stack, and prohibiting the development of damaging thermal gradients. The design of high temperature thermal insulation involves an analysis of radiative transfer in participating media (within the insulation materials), while the transfer of heat from the stack to the insulation and to the environment can be modeled as surface-to-surface radiation exchange.

Inclusion of radiative transfer in analysis of heat transfer entails a number of challenges, which are particular to thermal radiation modeling and not encountered in analysis of convective–conductive heat transfer. The first is the inherent complexity of the governing equations, which are integro-differential and, in general, depend on as many as seven independent variables (time, three position variables, two angular variables describing direction of propagation of radiation rays, and the wavelength). Further, the governing equations are non-linear, as the emissive power features a fourth-power dependence on temperature. Besides the difficulty associated with solving these equations, the accuracy of any analysis is

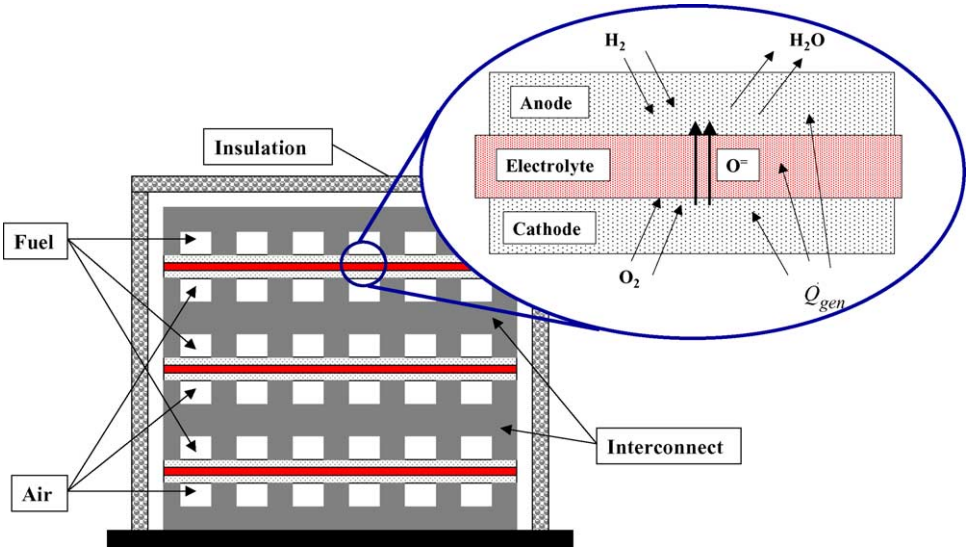

Fig. 1. Schematic of a planar SOFC stack consisting of numerous individual unit cells. Radiation effects are important on various levels: (1) within each individual cell, (2) between the cell stack and insulation, (3) within the insulation, and (4) between the insulation and surroundings.

always limited by the extent to which radiative properties are known. Unlike the thermophysical properties relevant to conduction or convection heat transfer, which are well behaved, rather well characterized, and usually weakly dependent on temperature, radiative properties are often highly (even erratically) dependent on wavelength of radiation and surface preparation, and a strong function of the temperature. Furthermore, in many cases limited experimental data exist for radiative properties, and even that is for the materials relevant to power generation and aerospace applications. Fortunately, in certain cases, making use of carefully justified simplifying assumptions renders these difficulties manageable and allows one to obtain results sufficiently accurate for engineering calculations. Even a simplified analysis can be very costly, however, increasing computational time requirements by an order of magnitude or more [6,11] as compared to the conductive–convective heat transfer calculations alone. This fact motivates us not only to discuss the existing modeling methodologies and simplifying assumptions for treating radiative heat transfer, but also to specify the conditions under which certain radiative effects could be neglected altogether.

2. Electrode/electrolyte (PEN) structure

2.1. Radiative properties

In general, the electrolyte and the porous electrodes of SOFCs are semitransparent materials; that is, they can absorb, scatter, and emit thermal radiation. For a linear medium, the spectral absorption coefficient (κ), refractive index (n), spectral scattering coefficient (σ_s), and the scattering phase function (Φ) provide a complete set of phenomenological properties required to model the propagation of radiative energy in the medium. In addition, emissivity (ε) and reflectivity (ρ) of the bounding interfaces must be provided in order to specify the boundary conditions [13]. Accurate knowledge of these properties, or the lack of it, as a function of the wavelength and temperature is currently the biggest obstacle to correctly predict radiative heat transfer in SOFC electrodes and electrolyte. Only recently, initial efforts have been made to experimentally measure some of these properties. Murthy and Fedorov [6] used FTIR spectrometer measurements of spectral normal transmittance and reflectance for a single crystal of yttria-stablized zirconia (YSZ) to compute its extinction coefficient and refractive index, but reported no information about scattering phase function. In a follow-up work [7], radiative properties of polycrystalline YSZ electrolyte were calculated based on FTIR measurements of the spectral normal transmittance and reflectance. The absorption coefficient was found to have a strong spectral dependence (see Table 1). Similarly, 200 μm thick samples of fully densified Ni-doped YSZ (anode) and strontium-doped $LaMnO_3$ (LSM) (cathode) were investigated and found to be completely opaque, which is indicative of a large extinction coefficient. However, extinction of radiation could be caused by either or both absorption and strong scattering of radiation; the latter may be especially significant because of the porous nature of the electrode samples. Unfortunately, FTIR transmission measurements do now allow one to discriminate between extinction mechanisms via absorption and scattering of thermal radiation, which is a significant limitation imposed on the extent of the modeling rigor that can be used in the analysis. Finally, it should also be mentioned that experimental data on radiative properties discussed above were taken at room temperature, and these properties may be quite different at the elevated temperatures (600–1000 °C) characteristic to SOFC operation.

Table 1
Absorption coefficient and refractive index of YSZ

Wavelength, λ (μm)	Absorption coefficient, κ (cm^{-1})	Refractive index
1.0	172	1.38
1.5	165	1.79
2.0	163	1.90
2.5	162	1.80
3.0	159	1.83
3.5	148	1.86
4.0	121	1.88
4.5	90	1.88
5.0	66	1.87
5.5	50	1.85
6.0	40	1.84
6.5	34	1.82
7.0	35	1.79
7.5	47	1.75
8.0	65	1.71
8.5	79	1.67
9.0	109	1.63
9.5	152	1.58
10.0	203	1.52

2.2. Modeling radiative transport

Modeling of thermal radiation propagation in participating media requires solution of the radiative transfer equation [13] (RTE), an integro-differential equation which cannot be solved analytically in its most complete form. It is convenient to write an RTE in terms of the spectral optical thickness, $\tau_\lambda = \int_0^s \beta_\lambda \, \mathrm{d}s$, which is a rescaled spatial variable, s, in the direction of radiation beam propagation with the spectral extinction coefficient, $\beta_\lambda = \kappa_\lambda + \sigma_\lambda$, acting as scaling factor. In quasi-steady state form, with the given change of variables, the RTE is,

$$\frac{\mathrm{d}I_\lambda}{\mathrm{d}\tau_\lambda} = -I_\lambda + (1-\omega_\lambda) I_{\mathrm{b}\lambda} + \frac{\omega_\lambda}{4\pi} \int_{4\pi} I(\hat{s}_i) \Phi(\hat{s}_i, \hat{s}) \, \mathrm{d}\Omega_i \qquad (1)$$

where I_λ is the spectral intensity of radiation, $I_{\mathrm{b}\lambda}$ the blackbody intensity of radiation (function of the local temperature), $\omega_\lambda = \sigma_\lambda/\beta_\lambda$ the single scattering albedo (ratio of radiation decay by scattering to the total extinction of radiation), and $\Phi(\hat{s}_i, \hat{s})$ is the scattering function, which upon integration over the entire hemisphere in Eq. (1) gives augmentation of radiation via in-scattering (i.e., redirection of radiation from

other directions to the given direction). The radiative heat flux at any point within the medium can be computed from the spectral intensity of radiation (after it is determined by solving Eq. (1)) by integration over all possible directions of radiation propagation as well as over the entire electromagnetic spectrum,

$$q_r = \int_0^\infty \int_{4\pi} I_\lambda(\hat{s})\hat{s}\, d\Omega\, d\lambda \tag{2}$$

Solving Eq. (1) in the most general case of a three-dimensional, spectrally dependent, absorbing–scattering–emitting medium is a formidable task even when it is done numerically. Therefore, it is beneficial to explore approximate solutions of the problem which are valid in the limit of some simplifying assumptions, provided those can be justified for the problem in hand. First of all, the typical SOFC unit cell geometry features very thin (high aspect ratio) layers of electrode and electrolyte materials arranged in either plane–parallel (planar design) or cylindrical/concentric (tubular design) fashion, thereby making a one-dimensional heat transfer approximation well justified. This reduction in dimensionality of the problem reduces the complexity significantly.

The experimental data suggest that SOFC electrodes are opaque and, therefore, volumetric radiation can be neglected or treated in the limit of the optically thick media approximation, for which the optical distance, $\tau_L = \beta L \gg 1$, if the extinction coefficient is known. In this case, the very simple, Rosseland approximation [13] can be invoked since the mean free path for photon propagation is short and radiation propagation can be treated as a diffusion process. On the other hand, the YSZ electrolyte appears to be optically thin [7] ($\tau_L \leq 1$), and in the case of a 1D, plane–parallel medium the Schuster–Schwartzchild two-flux approximation [13] can be used to reduce the RTE (Eq. (1)) to a second-order ODE for spectral radiative heat flux. In analyzing radiative transfer in the SOFC electrolyte, the two-flux approximation yielded a 10-fold reduction in computation CPU time compared to the most accurate discrete ordinates method of solving an RTE without losing much accuracy [6]. Further, details on the two-flux formulation for radiation propagation in the SOFC planar unit cell is given by references [6,7]. For tubular cell geometries, if the thickness of the electrolyte is sufficiently small compared to diameter of the tube, a one-dimensional planar solution of RTE may be used to obtain an approximate solution, but strictly speaking, the cylindrical coordinate formulation is required.

2.3. Coupling of radiation to overall energy conservation

In the optically thick case of SOFC electrodes, augmentation of total heat flux due to thermal radiation is accounted for by using an effective thermal conductivity, given by the sum of the intrinsic thermal conductivity of the medium and the Rosseland radiative "conductivity" defined as,

$$k_r = \frac{16n^2\sigma T^3}{3\beta} \tag{3}$$

where T is the absolute local temperature (K), σ the Stefan–Boltzmann constant ($5.67 \times 10^{-8}\,W\,m^{-2}\,K^4$), n the refractive index of the medium, and β is the spectrally averaged Rosseland-mean extinction coefficient of the medium $\frac{1}{\beta} = \frac{\pi}{4\sigma T^3}\int_0^\infty \frac{1}{\beta_\eta}\frac{dI_{b\eta}}{dT}d\eta$ ($\eta = 1/\lambda$ is the wavenumber). Radiation is thus coupled to overall energy conservation as,

$$q_{total}(z) = q_{cond}(z) + q_{rad}(z) = -k\frac{dT}{dz} - k_r\frac{dT}{dz} = -\underbrace{\left(k + \frac{16n^2\sigma T^3}{3\beta_r}\right)}_{\text{effective thermal conductivity}}\frac{dT}{dz} \tag{4}$$

However, caution must be exercised because this approximation does not perform well near boundaries where even an optically very thick medium is locally optically thin. A comparison of the radiative conductivity to the intrinsic thermal conductivity indicates the relative magnitudes of radiation and conduction heat fluxes. As shown in the analysis by Murthy and Fedorov [6], the radiative conductivity of the electrodes is much smaller than the overall thermal conductivity, implying that radiation in the electrodes could safely be neglected.

In the optically thin case of SOFC electrolyte, the two-flux approximation provides the radiative heat flux at every point within the medium. In order to couple radiation with other modes of heat transfer (only conduction in the case of the electrolyte), the divergence of the total radiative heat flux is added to the overall energy conservation equation as a heat sink,

$$S = -\nabla \cdot q_r \tag{5}$$

If *spectral* radiative heat flux [7] is calculated as a solution of the RTE, it must be integrated over the entire spectrum to obtain the *total* radiative heat flux, which is used in Eq. (5).

The relative importance of radiative heat transfer in the optically thin electrolyte depends on a number of parameters, with the thickness of the electrolyte layer and the temperatures at the boundaries being the most important. In general, the greater the temperature is and the thicker the layer is, the more significant the radiative transfer becomes as compared to heat conduction in electrolyte. This is because the radiative heat flux is scaled with temperature to the fourth power (unlike the linear dependence of the conductive heat flux), while conductive resistance to heat transfer increases linearly with the thickness of the conductive layer. Therefore, it is not surprising that Murthy and Fedorov [6] showed that thermal radiation through the electrolyte dramatically affected the operating temperature and voltage in a monolith-type cell with a thick, 500 μm electrolyte. More recently, with better radiative property information and for the state-of-the-art, anode-

supported planar cells with very thin (∼15 μm) electrolyte, the effect of radiation was found to be negligible compared to conduction in the solid [7].

As a general rule, in order to quickly determine whether or not to include radiation in the analysis, the magnitude of the maximum radiative heat flux can be compared to the magnitude of the conductive heat flux. The radiative heat flux at any point in a medium bounded by two temperatures, T_1 and T_2, cannot exceed the limit set by radiation exchange between two black walls separated by a radiatively transparent medium,

$$q_r = n^2\sigma(T_1^4 - T_2^4) \tag{6}$$

and the radiative heat flux will only be reduced from this value as a separating medium becomes absorbing. Thus, if this maximum radiative heat flux is much less than the average conductive heat flux given by the following expression for the layer whose thickness is L,

$$q_c = k\frac{T_1 - T_2}{L} \tag{7}$$

then the radiative heat transfer effects will be negligible. This scaling argument should only be used as a filter to eliminate unnecessary, costly computations, not as an analysis tool. We cannot stress enough how many simplifying assumptions are involved in the analyses presented above, and the reader should exercise these results with great care as they cannot be automatically extended to other geometries, configurations, or operating conditions.

3. Air/fuel channels

In this section, we consider radiative transfer in the flow channels which are used to supply the fuel (hydrogen or hydrocarbons) and oxidizer (air) to the cell PEN structure and are bounded by hot (emitting radiation) walls. In general, one needs to consider emission and reflection of radiation by the walls as well as its extinction (absorption and scattering) and emission by the flowing gases.

3.1. Radiative properties

Air mainly consists of simple non-polar nitrogen and oxygen molecules and, therefore, is non-interacting (transparent) with thermal radiation at the moderate pressures and temperatures found in SOFCs [13]. Therefore, no bulk extinction and emission of radiation take place, limiting the radiative transfer to surface-to-surface exchange of radiative energy. For the fuel channels, however, the analysis is more complicated due to the presence of the following participating species: H_2O, CO_2, CO, CH_4, and possibly, other hydrocarbons. Radiative properties of these gases are well established (even at high temperatures) and show very strong spectral, temperature, and pressure dependence [13]. Therefore, an accurate treatment of spectral emission and absorption by gases can quickly become very involved with more than a half of a dozen of advanced, competing models available, each of them still with somewhat limited range of validity.

Here, we are more interested in a simplified analysis in order to establish whether or not radiation transfer in gases should be considered at all or if gases can be treated as essentially non-participating medium as far as SOFC fuel flow channels are concerned. To this end, the concept of the Planck-mean absorption coefficient becomes very useful for this approximate back-of-the-envelope analysis. From the literature data (see, for example, Modest [13]) these spectrally averaged absorption coefficients are approximately: $0.1\,\mathrm{cm^{-1}\,bar^{-1}}$ for H_2O; $0.3\,\mathrm{cm^{-1}\,bar^{-1}}$ for CO_2 and CO; $0.4\,\mathrm{cm^{-1}\,bar^{-1}}$ for CH_4 at 600 °C. A quick calculation of the optical thickness of the fuel channel across its diameter (∼5 mm) for a typical fuel stream composition yields $\tau_L < 0.1$ at atmospheric pressure, leading to gas transmittance, $\mathrm{Tr} = \exp[-\tau_L]$, approaching unity—implying that the medium can be treated as transparent. Surface-to-surface radiation exchange is thus the only radiative transfer mode that must be considered in the flow channels of SOFC unit cells. From the property perspective, the only required input to this model is the emissivity of the relevant materials, which is not well known and can vary significantly depending on temperature and redox state. Finally, it should be noted that this conclusion is strictly valid for the air/fuel supply channels with very high aspect ratio only. Not surprisingly, the same conclusion was reached in the recent paper presented by VanderSteen and Pharoah [8] although several aspects of the analysis presented by these authors are not strictly accurate.

3.2. Modeling surface-to-surface radiative exchange

Here, we review the net radiosity method [13] for calculating the radiative heat flux between surfaces in a channel (planar and tubular cell) separated by a transparent medium, and comment on some simplifications that can be made to the analysis under certain conditions. As a first approximation, one can assume that the walls are opaque, gray, diffuse emitters, and reflectors of thermal radiation, especially in the absence of more detailed property data. However, in the case, when one of the walls is a porous surface of the electrode, this assumption may be questionable and the analysis becomes proportionately more complex. One way to avoid this difficulty is to assign an apparent emissivity and reflectivity to the porous electrode interface, which can be computed or measured by considering the entire porous electrode layer. By forming an enclosure based on the flow channel geometry (where all openings are closed by virtual black surfaces maintained at 0 K), the radiative heat flux at any point on the surface of the flow channel is given by,

$$\frac{q(\boldsymbol{r})}{\in(\boldsymbol{r})} - \int_A \left(\frac{1}{\in(\boldsymbol{r}')} - 1\right) q(\boldsymbol{r}')\,\mathrm{d}F_{\mathrm{d}A-\mathrm{d}A'} + H_0(\boldsymbol{r}) = E_b(\boldsymbol{r}) - \int_A E_b(\boldsymbol{r}')\,\mathrm{d}F_{\mathrm{d}A-\mathrm{d}A'} \tag{8}$$

where $dF_{dA-dA'}$ is the diffuse shape (view) factor between two surface elements dA and dA', ε the emissivity of the surface, $E_b = \sigma T^4$ the blackbody emissive power, and H_0 is incident radiation entering or leaving the enclosure through a virtual surface (can be used to couple analysis of the flow channel with radiation to/from the cell surrounding/manifolds). Notice that in order to solve Eq. (8) for heat flux, the temperature at every point in the enclosure must be known as well as the emissivity. However, the flow channels in the planar-type fuel cells typically have high aspect ratio ($L/d \sim 30$), and therefore, following the conclusions reached in papers [14–16], the walls can be treated as black surfaces with emissivity equal to 1. This greatly simplifies the analysis, and the radiative heat flux at any point on the channel walls can be expressed as,

$$q_r = E_b(\boldsymbol{r}) - \int_A E_b(\boldsymbol{r}')\, dF_{dA-dA'} - H_0(\boldsymbol{r}) \tag{9}$$

The view factor $dF_{dA-dA'}$ in Eqs. (8) and (9) physically represents the fraction of radiation leaving surface element dA that is incident on another surface element dA' without any intermediate reflections, i.e., via direct travel (see Fig. 2). View factors are geometric quantities which can be evaluated analytically, numerically, or by consulting tabulated values [13]. The view factors between elements on the channel walls and inlet/outlet elements diminish to zero very rapidly with distance from the end [15]. The view factors between elements at fixed axial positions (i.e., on top of each other) are relatively large, but the temperature differences between the wall surface elements at a given axial position are relatively small in a typical fuel cell. Thus, radiative heat flux is not expected to have a large effect on the average operating temperature of the cell, although some have indicated as much as a 30 °C decrease in maximum temperature and a flattening of the temperature profile with the inclusion of surface radiation in planar cell channels [8,11].

It is important to point out the fundamental difference between a tubular cell channel and planar cells in analyzing the flow channel radiation exchange. In the tubular cell, radiation exchange is between the surfaces of two concentric tubes, the air supply tube, and the porous support tube (Fig. 3), and the black surface approximation would not generally be appropriate. However, there does exist symmetry in the radial direction that allows the channel to be discretized into N isothermal slices unlike the channels in planar cells. Fig. 4 shows this schematically, and gives an indication of the view factors that should be calculated. Depending on geometry of the channel, some of these view factors may be negligible or vanish quickly in the axial direction.

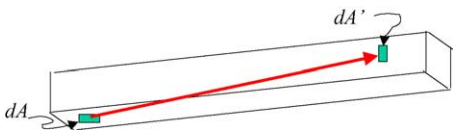

Fig. 2. Schematic to aid in view factor definition for two surface elements in a planar cell flow channel.

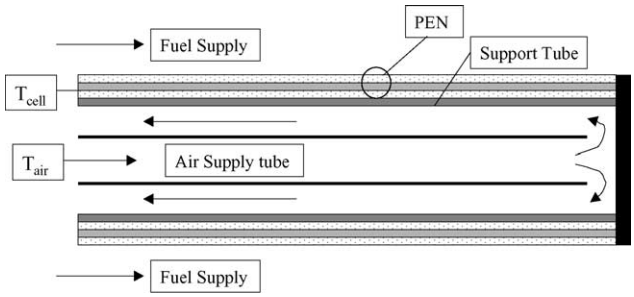

Fig. 3. In a tubular cell [9,10], thermal radiation from the outer supporting air tube to the air supply pipe is the dominant heat transfer mechanism due to the large temperature difference between the two surfaces.

Once again, this must be determined on a case-by-case basis.

3.3. Coupling of radiation to energy equation

Once radiative heat flux at the surface is calculated, it can be incorporated into overall energy conservation through the boundary conditions at the walls,

$$q_{conv} + q_{rad} = q_{cond} \rightarrow h(T_b - T_\infty) + q_{rad} = -k\left.\frac{\partial T}{\partial n}\right|_{boundary} \tag{10}$$

Comparison of the magnitude of the convective and radiative heat fluxes will give an indication of which heat transfer mode is dominant, and which, if any, can be neglected.

4. Insulation materials

4.1. Radiative properties

Recently, Spinnler et al. [17,18] published an excellent theoretical and experimental analysis of high temperature insulation for application to SOFC stacks. The insulation design considered by these authors featured multi-layer thermal insulations (MTIs), wherein highly reflective screens are separated by insulating, opaque spacers as shown in Fig. 5. The screens increase the overall thermal resistance

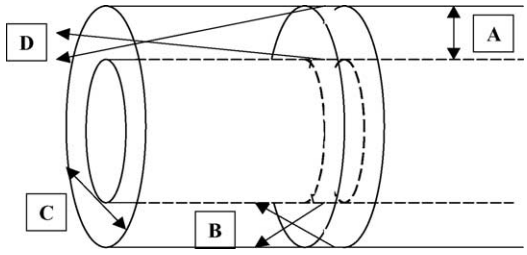

Fig. 4. View factor calculation for the isothermal slices on two concentric tubes: (A) the inner surface "sees" the outer surface of the same slice and vice versa, (B) both surfaces see other slices along the axial direction, (C) the outer surface sees itself, and (D) both surfaces of a given slice see the external environment.

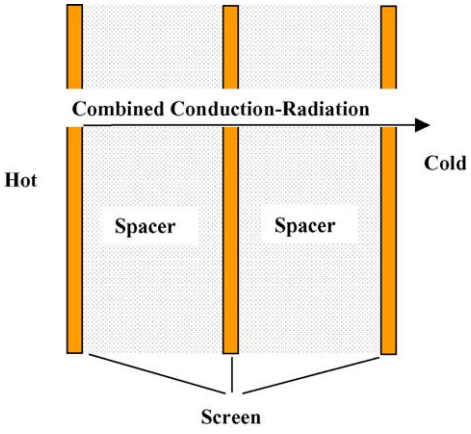

Fig. 5. Multi-layer thermal insulation wherein opaque, insulating spacer materials are separated by reflective screens which reduce the heat loss by back-reflecting thermal radiation [17,18].

of the MTI by reflecting thermal radiation back towards the hot side. Several screen materials such as gold, ceramic, and stainless steel have been considered with reflectivity ranging from high to low values, respectively. The spacer materials considered by the authors were of the fibrous (thermal conductivity, $k \sim 0.1$–$0.35\,\mathrm{W\,m^{-1}\,K^{-1}}$) and microporous ($k \sim 0.02$–$0.04\,\mathrm{W\,m^{-1}\,K^{-1}}$) type with known absorption and scattering characteristics. The goal of the analysis was to develop a thermal model for MTIs that predicts the experimentally measured effective thermal conductivity, given material selection and configuration.

4.2. Radiation model

The analysis was done in the limit of steady, one-dimensional conductive–radiative heat transfer in the plane–parallel layer of insulation. It was determined that the Rosseland diffusion approximation underestimates the influence of radiation screens, since the opaque spacer material is optically thin very near the screens. Thus, the RTE was still used to calculate radiative heat transfer in the optically thick spacers,

$$\cos\theta \frac{\mathrm{d}I}{\mathrm{d}s} = -\beta I + \kappa n^2 I_\mathrm{b} + \frac{\sigma}{2}\int_0^\pi I(\hat{s}, \theta')\,\sin\theta'\,\mathrm{d}\theta' \qquad (11)$$

In order to solve the RTE, the scaling model of Lee and Buckius [19,20], which converts a scattering radiation problem into a non-scattering one, was used. In this elegant approach, the scattering coefficient is set to zero and the transmission and reflection coefficients are scaled, assuming linear scattering in an optically thin layer, as

$$\tau_{\mathrm{L},\beta} = (1-\omega)\tau_\mathrm{L} \quad \text{and} \quad \rho_\beta = 1 - \frac{2}{\frac{3}{4}\tau_\mathrm{L}\omega + 2} \qquad (12)$$

A further simplifying technique was to split up each layer of spacer material into N optically thin, isothermal layers, which are irradiated and emit radiation from both sides. In this manner, the transmittance, reflectance, and emittance of each layer were calculated independently and added together to yield the total radiative heat flux. The heat flux was then coupled to the energy equation in the solid via a source term,

$$\frac{\mathrm{d}}{\mathrm{d}x}\left[-k_\mathrm{c}\frac{\mathrm{d}T}{\mathrm{d}x} + q_\mathrm{r}\right] = 0 \qquad (13)$$

The theoretical model predictions compared favorably with results in the literature for highly scattering materials, but not so well for purely absorbing materials.

4.3. Experimental results

The theoretical predictions were also compared to experimental data obtained by the authors [17,18]. Test MTIs 30 mm in thickness were constructed with screens (four equally spaced) and without screens. The screens were stainless steel (Cr 22 A15Y), gold, or ceramic (Al_2O_3). The spacer materials tested were Isotherm 1000 (Frenzelit), HT 1000 (Klevers), Saffil (ICI), and Super G (Microtherm). Theoretical calculations of temperature dependent, effective thermal conductivity fit the experimental data within 10% except for the case of highly absorbing spacer materials.

In general, the presence of the screens dramatically lowers the effective thermal conductivity of the MTI, by as much as 50% in some cases. Also, it was shown that effective conductivity decreases with a decrease in screen emissivity (gold screens performed best). As expected, use of higher opacity spacer materials such as Microtherm Super G resulted in lower effective thermal conductivity. Overall, this work [17,18] provides a sound theoretical and experimentally validated basis for the design and application of multi-layer thermal insulation and can be recommended for use in design analysis of other thermal insulation materials for SOFCs.

5. Radiation from stack to environment

Effective stack thermal management is a requirement for maintaining uniform operating conditions across the stack and thus preserving stack efficiency. For example, if cells near the edge of the stack are not properly insulated, their performance can vary from the stack average causing variations in cell voltage. Heat loss from the edges also has the potential to induce damaging thermal gradients within cells. In addition, SOFC-based power plant design will require the outer surface of the insulation to be maintained at some safe, prescribed temperature [21]. These considerations make thermal modeling of the stack to environment critical, and because of high operating temperatures, thermal radiation should be given special treatment.

A first-order simplifying approximation in modeling the stack would be to treat the outer surface of the stack as isothermal, exchanging heat with an isothermal inner surface of the insulation [21]. However, this is clearly not the case for some configurations of cells (co-flow, counter-flow), which exhibit highly non-isothermal behavior along the flow direction. It

would be ideal to preserve this same temperature profile on the inner surface of the insulation, so as not to disturb the outer cells. In fact, a single cell can become completely isothermal if it is allowed to exchange thermal radiation with an isothermal enclosure [22]. This temperature non-uniformity would then propagate into the stack, affecting overall performance. Our literature review indicates that little has been reported about the interaction between stack and insulation and on the role of radiation heat transfer in minimizing heat losses from the stack. The methods for detailed treatment of radiation heat transfer in stack thermal management have already been covered in this paper and they are equally applicable to treatment of stack-to-environment radiation heat transfer. We can only emphasize again that the choice of the model and implementation will depend on the geometry, flow configuration, and composition of the gas mixture, choice of insulating material, and prescribed external temperature of the insulation.

6. Concluding remarks

Radiation heat transfer in SOFC components and materials has been reviewed with a goal of providing guidelines on how to identify the proper radiation models for different cases. Simplifying assumptions and simple scaling laws have been introduced, where applicable, to provide guidance and reduce costly computations. Radiation in participating media and surface-to-surface radiation exchange have been considered both within the unit cell and at the stack level. It was demonstrated that only careful treatment of these radiative regimes would enable an accurate prediction of temperature fields and operating conditions. Although our scaling analysis indicates that certain radiative regimes may be negligible in the heat transfer analysis of SOFCs, we hope that the reader has also developed a clear understanding of the assumptions that led to these conclusions, which may or may not be valid in each specific case encountered in a growing family of new SOFC designs and configurations. An ongoing need is radiative property information – both bulk and surface properties at the high temperatures relevant to SOFC – which is currently incomplete and yet to be determined as new materials are developed.

Acknowledgements

The support of this work by DOE through the Phase II SECA program and DOD through the NDSEG fellowship program is acknowledged and appreciated.

References

[1] Fuel Cell Handbook, fifth ed., EG&G Services, National Technical Information Service, U.S. Department of Commerce, 2000.
[2] A. Hirano, M. Suzuki, M. Ippommatsu, J. Electrochem. Soc. 139 (10) (1992) 2744–2751.
[3] S. Ahmed, C. McPheeters, R. Kumar, J. Electrochem. Soc. 138 (9) (1991) 2712–2718.
[4] N.F. Bessette, W.J. Wepfer, Thermodynamics and the Design Analysis and Improvement of Energy Systems 27, ASME AES Publications, 1992, pp. 69–80.
[5] J. Hartvigsen, S. Elangovan, A. Khandkar, Proc. Sci. Tech. Zirconia V, 1993, pp. 682–693.
[6] S. Murthy, A.G. Fedorov, J. Power Sources 124 (2003) 453–458.
[7] D.L. Damm, A.G. Fedorov, Proc. ASME Int. Mech. Eng. Congress Expo., Anaheim, CA, 2004, in press.
[8] J.D.J. VanderSteen, J.G. Pharoah, Proc. Fuel Cell Sci. Eng. Tech., ASME, Rochester, NY, 2004, pp. 483–490.
[9] P.W. Li, L. Schaefer, M.K. Chyu, J. Heat Transfer 126 (2004) 219–229.
[10] C. Haynes, W.J. Wepfer, Int. J. Hydrogen Energy 26 (2001) 369–379.
[11] H. Yakabe, T. Ogiwara, M. Hishinuma, I. Yasuda, J. Power Sources 102 (2001) 144–154.
[12] A.C. Burt, I.B. Celik, R.S. Gemmen, A.V. Smirnov, J. Power Sources 126 (2004) 76–87.
[13] M.F. Modest, Radiative Heat Transfer, second ed., Academic Press, New York, 2003.
[14] A.L. Boehman, AIChE J. 44 (12) (1998) 2745–2755.
[15] N.S. Kaisare, J.H. Lee, A.G. Fedorov, AIChE J., 2005, in press.
[16] X. Fu, R. Viskanta, J.P. Gore, J. ThermoPhys. Heat Transfer 12 (2) (1998) 164–171.
[17] M. Spinnler, E.R.F. Winter, R. Viskanta, Int. J. Heat Mass Transfer 47 (2004) 1305–1312.
[18] M. Spinnler, E.R.F. Winter, R. Viskanta, J. Quant. Spectrosc. Radiat. Transfer 84 (2004) 477–491.
[19] H. Lee, R.O. Buckius, Int. J. Heat Mass Transfer 26 (1983) 1055–1062.
[20] H. Lee, R.O. Buckius, High Temp. High Press. 17 (1985) 626–632.
[21] L. Petruzzi, S. Cocchi, F. Fineschi, J. Power Sources 118 (2003) 96–107.
[22] M. Iwata, T. Hikosaka, M. Morita, T. Iwanari, K. Ito, K. Onada, Y. Esaki, Y. Sakaki, S. Nagata, Solid State Ionics 132 (2000) 297–308.